Full-Wave Analysis of Radiating Planar Resonators with the Method of Lines

Achim Dreher, *Member, IEEE,* and Reinhold Pregla, *Senior Member, IEEE*

***Abstract*—The method of lines (MoL) is extended to analyze radiating planar resonators by the use of absorbing boundary conditions. For stratified layers, an equivalent network is derived to set up a system equation by simple multiplication of hybrid matrices. As an example, the complex resonant frequency of a microstrip patch is computed and compared to results achieved with the integral equation method in spectral domain. The radiation in the near-field region is depicted by a vector plot of the energy flow, given by the real part of the Poynting vector.**

I. Introduction

The full-wave analysis of open planar microstrip patches without any approximations is a difficult task. It usually involves extensive mathematical preparations that become even more complicated if the complex resonant frequency, as a solution of an eigenvalue problem, must be determined [1], [6].

On the other hand, the method of lines (MoL) is a simple and efficient tool for the analysis of planar waveguide structures with multiple layers and arbitrary shape. The Helmholtz equation is discretized in two directions of coordinates, whereas an analytical solution is used in the remaining direction. Because of the relation to the discrete Fourier transform, exact results are achieved with just a few lines [2].

In this paper, the MoL is extended to analyze radiating microstrip patches. To limit the area of discretization, the structure is enclosed by walls on which absorbing boundary conditions are used to simulate the free space [7], [9]. Since the discretization is performed in two dimensions, only four of these walls are necessary. Structures with multiple layers can be treated as series connection of two-ports represented by hybrid matrices. This procedure is similar to the immittance approach in spectral domain, but the splitting into TE- and TM-modes is not necessary.

As an example, the complex resonant frequency of a rectangular microstrip patch (Fig. 1) is computed and compared to results obtained by the integral equation method. The energy flow, given by the real part of the Poynting vector, is determined in the whole discretized area.

II. Analysis

A. Absorbing Boundaries and Discretization

Assuming a time dependence exp $(j\omega t)$, the wave equation, normalized by k_0, for the two independent field components

Manuscript received August 21, 1992; revised December 11, 1992.
The authors are with FernUniversität, Postfach 940, W-5800 Hagen, Germany.
IEEE Log Number 9210206.

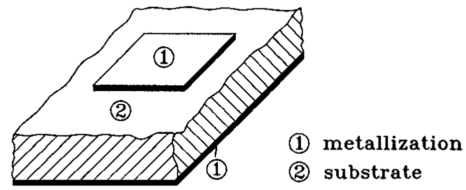

Fig. 1. Simple microstrip patch.

e_z, h_z can be written as

$$L\psi = \left(D_{\bar{x}}^2 + D_{\bar{y}}^2 + D_{\bar{z}}^2 + \varepsilon_r\right)\psi = 0 \tag{1}$$

with

$$D_{\bar{x}}^2 \equiv \frac{\partial^2}{\partial \bar{x}^2} \qquad D_{\bar{y}}^2 \equiv \frac{\partial^2}{\partial \bar{y}^2} \qquad D_{\bar{z}}^2 \equiv \frac{\partial^2}{\partial \bar{z}^2}. \tag{2}$$

To limit the area of discretization, the structure must be enclosed by walls as shown in Fig. 2 and, owing to the radiation, these walls must simulate the free space to avoid reflections. This can be achieved by the use of absorbing boundary conditions (ABC) for the field components in this place [9]. To this end, the Helmholtz operator L is factored such that

$$L\psi = L^+L^-\psi = 0 \tag{3}$$

from which follow the boundary conditions

$$L_x^{\pm}\psi = 0 \qquad L_z^{\pm}\psi = 0 \tag{4}$$

with

$$\begin{aligned} L_x^{\pm} &= D_{\bar{x}} \pm j\sqrt{\varepsilon_r}\sqrt{1 + s_{\overline{yz}}^2} \\ s_{\overline{yz}}^2 &= \frac{1}{\varepsilon_r}\left(D_{\bar{y}}^2 + D_{\bar{z}}^2\right) \end{aligned} \tag{5}$$

in x-direction and

$$\begin{aligned} L_z^{\pm} &= D_{\bar{z}} \pm j\sqrt{\varepsilon_r}\sqrt{1 + s_{\overline{xy}}^2} \\ s_{\overline{xy}}^2 &= \frac{1}{\varepsilon_r}\left(D_{\bar{x}}^2 + D_{\bar{y}}^2\right) \end{aligned} \tag{6}$$

in z-direction. The plus sign is related to waves traveling in the positive, the minus sign to those traveling in the negative direction of coordinates. For a unique solution, the sign must be chosen properly at each wall so that only waves incident from the interior of the enclosed structure are admitted.

Unfortunately, due to the radical, the boundary conditions in (5) and (6) are nonlocal, so they cannot be applied directly

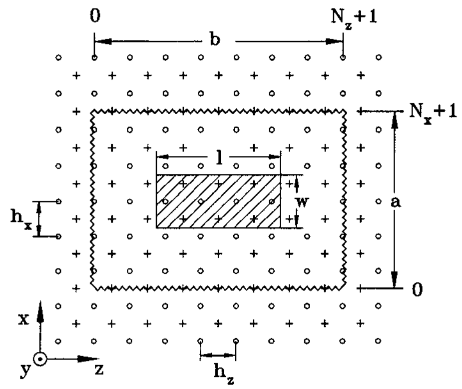

Fig. 2. Microstrip patch with discretization lines and absorbing boundaries.

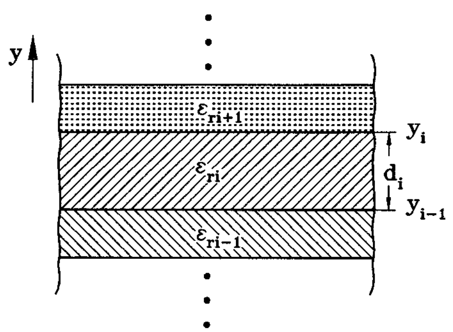

Fig. 3. Stratified dielectric with corresponding notations.

to the method of lines. The radical is therefore approximated by a polynomial of the form

$$\sqrt{1+s^2} \approx p_0 + p_2 s^2 \tag{7}$$

on the interval $s \in [-j, j]$, in which the parameters p_0 and p_2 are determined by the method of approximation and must fulfill the relationship

$$p_2 \le p_0 \le \frac{1}{4p_2} + p_2 \tag{8}$$

to meet the demand for an outgoing wave [6]. From now on, the absorbing boundaries are no longer ideal. Their reflection coefficient is a function of the angle of incidence [7], [10]. The boundary conditions can now be written as

$$L_x'^{\pm}\psi = 0 \qquad L_z'^{\pm}\psi = 0 \tag{9}$$

with

$$\begin{aligned} L_x'^{\pm} &= D_{\bar{y}}^2 + D_{\bar{z}}^2 \mp j\,\frac{\sqrt{\varepsilon_r}}{p_{x2}}\,D_{\bar{x}} + \varepsilon_r\,\frac{p_{x0}}{p_{x2}} \\ L_z'^{\pm} &= D_{\bar{y}}^2 + D_{\bar{x}}^2 \mp j\,\frac{\sqrt{\varepsilon_r}}{p_{z2}}\,D_{\bar{z}} + \varepsilon_r\,\frac{p_{z0}}{p_{z2}}. \end{aligned} \tag{10}$$

In the method of lines, the discretization of the wave equation for the field components e_z and h_z is performed with a set of two line systems shifted by half the discretization distance $\mathrm{h}_{x,z}$ (Fig. 2) [3] and, in the case of electric or magnetic walls, dual boundary conditions have been used to set up a system matrix in an elegant way [4].

To keep this advantageous procedure, dual boundary conditions have to be derived for the absorbing boundaries too. For this reason, the operator equations (9) are applied to the tangential field components e_z, e_y and e_x, e_y, respectively, resulting in

$$L_x'^{\pm} e_z = 0 \qquad L_x'^{\pm}\,\frac{\partial h_z}{\partial \bar{x}} = 0 \tag{11}$$

on walls parallel to the z-axis and

$$L_z'^{\pm}\,\frac{\partial e_z}{\partial \bar{z}} = 0 \qquad L_z'^{\pm} h_z = 0 \tag{12}$$

on walls parallel to the x-axis [6].

Combining (1) with (11) for the field component e_z and (1) with (12) for h_z respectively, the ordinary differential equations

$$\left(D_{\bar{x}}^2 \pm j\,\frac{\sqrt{\varepsilon_r}}{p_{x2}}\,D_{\bar{x}} - \left(\frac{p_{x0}}{p_{x2}} - 1\right)\varepsilon_r\right) e_z = 0 \tag{13}$$

$$\left(D_{\bar{z}}^2 \pm j\,\frac{\sqrt{\varepsilon_r}}{p_{z2}}\,D_{\bar{z}} - \left(\frac{p_{z0}}{p_{z2}} - 1\right)\varepsilon_r\right) h_z = 0 \tag{14}$$

are obtained. Their solutions result in the propagation constants of waves not being reflected by the absorbing wall. The accompanying angles of incidence, following from (13), e.g., are [6]

$$\cos\Theta_{1,2} = \frac{1}{2p_{x2}}\left(1 \pm \sqrt{1 - 4p_{x2}(p_{x0} - p_{x2})}\right). \tag{15}$$

From the discretized form of (13) and (14), the components on the walls can be determined as

$$e_{z0} = -a_x e_{z1} + b_x e_{z2} \tag{16}$$

$$e_{zN_x+1} = -a_x e_{zN_x} + b_x e_{zN_x-1} \tag{17}$$

$$h_{z0} = -a_z h_{z1} + b_z h_{z2} \tag{18}$$

$$h_{zN_z+1} = -a_z h_{zN_z} + b_z h_{zN_z-1} \tag{19}$$

with

$$\begin{aligned} a_{x,z} &= -2\,\frac{2p_{x,z2} + (p_{x,z0} - p_{x,z2})n_{x,z}^2}{2p_{x,z2} + jn_{x,z}} \\ b_{x,z} &= -\frac{2p_{x,z2} - jn_{x,z}}{2p_{x,z2} + jn_{x,z}} \qquad n_{x,z} = \bar{\mathrm{h}}_{x,z}\sqrt{\varepsilon_r} \end{aligned} \tag{20}$$

and, in this way, the boundary conditions are included in the difference operators [7], [8].

Due to the formulation of dual boundary conditions, the second derivatives are given by

$$\bar{\mathrm{h}}_x^2\,\frac{\partial^2 e_z}{\partial \bar{x}^2} \rightarrow \boldsymbol{D}_{xh}\boldsymbol{D}_{xe}\mathrm{E}_z = -\boldsymbol{P}_{xe}\mathrm{E}_z \tag{21}$$

$$\bar{\mathrm{h}}_x^2\,\frac{\partial^2 h_z}{\partial \bar{x}^2} \rightarrow \boldsymbol{D}_{xe}\boldsymbol{D}_{xh}\mathrm{H}_z = -\boldsymbol{P}_{xh}\mathrm{H}_z\,. \tag{22}$$

Similar representations can be found for the matrices $\boldsymbol{P}_{ze,h}$. The remaining boundary conditions for the derivatives of h_z and e_z in (11) and (12), respectively, are now fulfilled automatically.

Since the operators are independent in both directions of coordinates, their two-dimensional form can be obtained by using the Kronecker product [5]

$$\begin{aligned} \boldsymbol{D}_x &\rightarrow \widehat{\boldsymbol{D}}_x = \boldsymbol{I}_z \otimes \boldsymbol{D}_x \\ \boldsymbol{D}_z &\rightarrow \widehat{\boldsymbol{D}}_z = \boldsymbol{D}_z \otimes \boldsymbol{I}_x\,. \end{aligned} \tag{23}$$

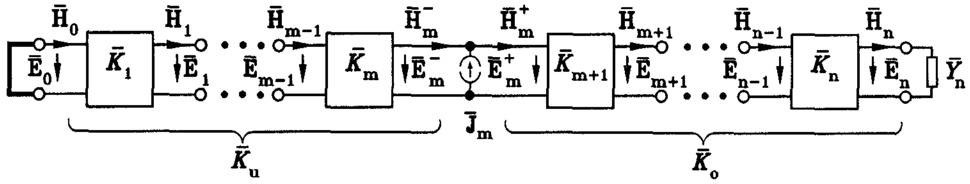

Fig. 4. Equivalent two-port representation of the stratified dielectric.

Depending on the order of operation, the dimensions of the identity matrices $\boldsymbol{I}_{x,z}$ have to be chosen properly, since the derivatives of the discretized components do not coincide with the corresponding line system.

B. Transformation

The discretized wave equation

$$\left(\hat{\boldsymbol{I}} D_{\bar{y}}^2 - \hat{\overline{\boldsymbol{P}}}_x - \hat{\overline{\boldsymbol{P}}}_z + \varepsilon_r \hat{\boldsymbol{I}}\right)\boldsymbol{\Psi} = \mathbf{0} \tag{24}$$

is transformed by

$$\boldsymbol{\Psi} = \hat{\boldsymbol{T}}\overline{\boldsymbol{\Psi}} \tag{25}$$

to get a system of uncoupled ordinary differential equations

$$\left(\hat{\boldsymbol{I}} D_{\bar{y}}^2 - \hat{k}_{\bar{y}}^2\right)\overline{\boldsymbol{\Psi}} = \mathbf{0}\,. \tag{26}$$

$\hat{\boldsymbol{T}}$ is the transformation matrix for the two-dimensional case given by

$$\hat{\boldsymbol{T}} = \boldsymbol{T}_z \otimes \boldsymbol{T}_x \tag{27}$$

and $\boldsymbol{T}_{x,z}$ are the eigenvectors of $\overline{\boldsymbol{P}}_{x,z} = \overline{\mathrm{h}}_{x,z}^{-2}\boldsymbol{P}_{x,z}$ according to

$$\boldsymbol{T}_{x,z}^{-1}\overline{\boldsymbol{P}}_{x,z}\boldsymbol{T}_{x,z} = \overline{\boldsymbol{\lambda}}_{x,z}^2\,. \tag{28}$$

Eigenvalues $\overline{\boldsymbol{\lambda}}_{x,z}^2$ and transformation matrices $\boldsymbol{T}_{x,z}$ are calculated numerically using appropriate standard software [12]. The numerical effort is minimal because their dimensions are determined by the number of lines in only one direction.

The two-dimensional eigenvalues are

$$\hat{\overline{\boldsymbol{\lambda}}}_x^2 = \boldsymbol{I}_z \otimes \overline{\boldsymbol{\lambda}}_x^2 \qquad \hat{\overline{\boldsymbol{\lambda}}}_z^2 = \overline{\boldsymbol{\lambda}}_z^2 \otimes \boldsymbol{I}_x \tag{29}$$

so that

$$\hat{k}_{\bar{y}}^2 = \hat{\overline{\boldsymbol{\lambda}}}_x^2 + \hat{\overline{\boldsymbol{\lambda}}}_z^2 - \varepsilon_r \hat{\boldsymbol{I}}\,. \tag{30}$$

Owing to (21) and (22), there exists a close connection between eigenvalues and transformed difference operators on both line systems [7], [8].

Suitable solutions of (26) are

$$\overline{\boldsymbol{\Psi}} = \cosh \hat{k}_{\bar{y}}\bar{y} \cdot \mathrm{A} + \sinh \hat{k}_{\bar{y}}\bar{y} \cdot \mathrm{B} \tag{31}$$

within the layers, and

$$\overline{\boldsymbol{\Psi}} = e^{-\hat{k}_{\bar{y}}\bar{y}} \cdot \mathbf{A}' \tag{32}$$

for the open top layer. In the latter case, the sign of the radical, following from (30) for $\hat{k}_{\bar{y}}$, must be chosen such that

$$\boldsymbol{T}\{k_0 k_{\bar{y}ij}\} > 0 \tag{33}$$

to get an outgoing wave only.

C. System Equation

The derivation of a system equation is done in the same way, as described in [2], and after some algebraic manipulations a hybrid matrix is obtained linking the tangential field components at both interfaces of an arbitrary dielectric layer (Fig. 3),

$$\begin{bmatrix}\overline{\mathbf{E}}_i\\ \overline{\mathbf{H}}_i\end{bmatrix} = \begin{bmatrix}\overline{\mathbf{V}}_i & \overline{\mathbf{Z}}_i\\ \overline{\mathbf{Y}}_i & \overline{\mathbf{V}}_i\end{bmatrix}\begin{bmatrix}\overline{\mathbf{E}}_{i-1}\\ \overline{\mathbf{H}}_{i-1}\end{bmatrix} \tag{34}$$

with

$$\overline{\mathbf{H}}_i = \eta_0\begin{bmatrix}\overline{\mathbf{H}}_{zi}\\ -\overline{\mathbf{H}}_{xi}\end{bmatrix} \qquad \overline{\mathbf{E}}_i = j\begin{bmatrix}\overline{\mathbf{E}}_{xi}\\ \overline{\mathbf{E}}_{zi}\end{bmatrix}. \tag{35}$$

At the interface to the open top layer n the relation between the tangential field components is

$$\overline{\mathbf{H}}_n = \overline{\mathbf{Y}}_n\overline{\mathbf{E}}_n \tag{36}$$

with

$$\overline{\boldsymbol{Y}}_n = \begin{bmatrix}\hat{k}_{\bar{y}h}^{-1} & \mathbf{0}\\ \mathbf{0} & \hat{k}_{\bar{y}e}^{-1}\end{bmatrix}\begin{bmatrix}-\hat{\varepsilon}_{zh} & \hat{\overline{\delta}}_{eh}\\ \hat{\overline{\delta}}_{he} & -\hat{\varepsilon}_{xe}\end{bmatrix}. \tag{37}$$

Herein, $\hat{\overline{\delta}}_{eh}$ and $\hat{\overline{\delta}}_{he}$ are the transformed difference operators. More details of the definitions of all quantities can be found in [7] and [2]. Notice, however, that some changes have been made to the vectors $\overline{\mathbf{H}}_i$ and $\overline{\mathbf{E}}_i$.

Due to the continuity of the tangential field components at the interfaces, the stratified structure can be represented by a series connection of two-ports (Fig. 4) with a short ($\overline{\mathrm{E}}_0 = \mathbf{0}$) for the metallization at the bottom of the structure and a termination with an admittance $\overline{\boldsymbol{Y}}_n$ at the top.

Cascading the matrices by simple multiplication yields

$$\overline{\mathrm{F}}_m^- = \overline{\boldsymbol{K}}_u\overline{\mathrm{F}}_0 \qquad \overline{\mathrm{F}}_n = \overline{\boldsymbol{K}}_o\overline{\mathrm{F}}_m^+ \tag{38}$$

with

$$\overline{\boldsymbol{K}}_u = \prod_{i=1}^{m}\overline{\boldsymbol{K}}_i \qquad \overline{\boldsymbol{K}}_o = \prod_{i=m+1}^{n}\overline{\boldsymbol{K}}_i$$

$$\overline{\mathbf{F}}_i = \begin{bmatrix}\overline{\mathbf{E}}_i\\ \overline{\mathbf{H}}_i\end{bmatrix} \qquad \overline{\boldsymbol{K}}_i = \begin{bmatrix}\overline{\boldsymbol{V}}_i & \overline{\boldsymbol{Z}}_i\\ \overline{\boldsymbol{Y}}_i & \overline{\boldsymbol{V}}_i\end{bmatrix}. \tag{39}$$

With the inclusion of the terminations, the tangential field components on the lower (−) and the upper (+) side of the interface m with metallization are related by

$$\overline{\mathbf{H}}_m^- = -\overline{\boldsymbol{Y}}_u\overline{\mathbf{E}}_m^- \tag{40}$$

$$\overline{\mathbf{H}}_m^+ = -\overline{\boldsymbol{Y}}_o\overline{\mathbf{E}}_m^+ \tag{41}$$

with

$$\overline{\boldsymbol{Y}}_u = -\overline{\boldsymbol{K}}_{u22}\overline{\boldsymbol{K}}_{u12}^{-1} \tag{42}$$

$$\overline{\boldsymbol{Y}}_o = \left(\overline{\boldsymbol{K}}_{o22} - \overline{\boldsymbol{Y}}_n\overline{\boldsymbol{K}}_{o12}\right)^{-1}\left(\overline{\boldsymbol{Y}}_n\overline{\boldsymbol{K}}_{o11} - \overline{\boldsymbol{K}}_{o21}\right). \tag{43}$$

Finally, the continuity equations for the tangential field components in this interface,

$$\overline{\mathbf{E}}_m^+ = \overline{\mathbf{E}}_m^- \qquad \overline{\mathbf{H}}_m^+ - \overline{\mathbf{H}}_m^- = \overline{\mathbf{J}}_m = \eta_0\begin{bmatrix}\overline{\mathbf{J}}_{xm}\\ \overline{\mathbf{J}}_{zm}\end{bmatrix} \tag{44}$$

must be taken into account and the system equation

$$\overline{\boldsymbol{Z}}\cdot\overline{\mathbf{J}}_m = \overline{\mathbf{E}}_m \tag{45}$$

with $\overline{\boldsymbol{Z}} = \left(\overline{\boldsymbol{Y}}_u + \overline{\boldsymbol{Y}}_o\right)^{-1}$ in the transform domain able to be formulated. To obtain an eigenvalue problem, (45) is transformed back to spatial domain, and the condition that the tangential electric field components must vanish on the patch leads to

$$\boldsymbol{Z}_{\text{red}}\mathrm{J}_{\text{red}} = \mathbf{0} \tag{46}$$

with a reduced system matrix $\boldsymbol{Z}_{\text{red}}$. This equation has to be solved for the complex resonant frequency $\omega = \omega' + j\omega''$.

In general, the transformation matrices are different for each layer. In this case, the hybrid matrices are transformed back to spatial domain before cascading, according to

$$\boldsymbol{K}_i = \boldsymbol{T}_i\overline{\boldsymbol{K}}_i\boldsymbol{T}_i^{-1} \tag{47}$$

with

$$\boldsymbol{T}_i = \text{Diag}\left(\tilde{\boldsymbol{T}}_i, \tilde{\boldsymbol{T}}_i\right) \qquad \tilde{\boldsymbol{T}}_i = \text{Diag}\left(\hat{\boldsymbol{T}}_{hi}, \hat{\boldsymbol{T}}_{ei}\right). \tag{48}$$

D. Radiation

The radiated power is given by the real part of the Poynting vector

$$\mathrm{p}_r = \Re\{e\times\mathrm{h}^*\}. \tag{49}$$

Since, in the method of lines, the field quantities are obtained in discretized form, the components of the Poynting vector are

$$\begin{aligned}\mathbf{P}_x &= \mathbf{E}_y\cdot\mathbf{H}_z^* - \mathbf{E}_z\cdot\mathbf{H}_y^*\\ \mathbf{P}_y &= \mathbf{E}_z\cdot\mathbf{H}_x^* - \mathbf{E}_x\cdot\mathbf{H}_z^*\\ \mathbf{P}_z &= \mathbf{E}_x\cdot\mathbf{H}_y^* - \mathbf{E}_y\cdot\mathbf{H}_x^*.\end{aligned} \tag{50}$$

The dot $(\cdot)$ means multiplication according to the Hadamard product of vectors [11]

$$\mathbf{A}\cdot\mathbf{B} = (a_i b_i). \tag{51}$$

This multiplication has to be performed at the same locus, so that interpolations are necessary due to the shifting of the line systems.

It can be shown that the imaginary part of the complex resonant frequency, which is obtained as a solution of a radiating system with no independent sources, must be positive, resulting in a spatially growing wave [6], whereas the amplitude of the current on the patch decreases with time. To compute the radiation property, a constant in time energy flow must be assumed. So, in the following, the imaginary part of ω is set to zero. This means, physically, that the eigensolutions form an impressed source to compensate for radiation losses.

From the system equation follows the eigenvector $\mathbf{J}_m$ which is transformed back to spectral domain to determine the field components $\overline{\mathbf{E}}_m$ in the plane of the patch. By means of the hybrid matrices (34), (40), and (41), the tangential field components in all interfaces of the layers are known.

The normal components $\overline{\mathrm{H}}_y$ and $\overline{\mathrm{E}}_y$ can be derived in the following way. From Maxwell's equation

$$\nabla\times\mathrm{e} = -j\omega\mu\mathrm{h} \tag{52}$$

follows

$$\eta_0 h_y = j\left(\frac{\partial}{\partial\overline{z}}e_x - \frac{\partial}{\partial\overline{x}}e_z\right). \tag{53}$$

Discretization and transformation leads to

$$\eta_0\overline{\mathbf{H}}_y = j\left(\hat{\overline{\boldsymbol{\delta}}}_{zh}\overline{\mathbf{E}}_x - \hat{\overline{\boldsymbol{\delta}}}_{xe}\overline{\mathbf{E}}_z\right). \tag{54}$$

In the same way, starting from

$$\nabla\times\mathrm{h} = j\omega\varepsilon_0\varepsilon_{ri}\mathrm{e} \tag{55}$$

the relation

$$\overline{\mathbf{E}}_y = j\,\frac{\eta_0}{\varepsilon_{ri}}\left(\hat{\overline{\boldsymbol{\delta}}}_{xh}\overline{\mathbf{H}}_z - \hat{\overline{\boldsymbol{\delta}}}_{ze}\overline{\mathbf{H}}_x\right) \tag{56}$$

can be obtained.

The y-dependence of all field components in spectral domain along the corresponding lines within the ith layer results from (31) by eliminating the unknown coefficient vectors

$$\overline{\mathbf{F}}(y) = \hat{\boldsymbol{\alpha}}\left(\hat{\boldsymbol{S}}_1\overline{\mathbf{F}}_{i-1} + \hat{\boldsymbol{S}}_2\overline{\mathbf{F}}_i\right) \tag{57}$$

with

$$\hat{\boldsymbol{\alpha}} = \left(\hat{\boldsymbol{k}}_{\overline{y}}\sinh\hat{\boldsymbol{k}}_{\overline{y}}\overline{d}_i\right)^{-1} \tag{58}$$

$$\hat{\boldsymbol{S}}_1 = \hat{\boldsymbol{k}}_{\overline{y}}\left(\sinh\hat{\boldsymbol{k}}_{\overline{y}}(\overline{y}_i - \overline{y})\right) \tag{59}$$

$$\hat{\boldsymbol{S}}_2 = \hat{\boldsymbol{k}}_{\overline{y}}\left(\sinh\hat{\boldsymbol{k}}_{\overline{y}}(\overline{y} - \overline{y}_{i-1})\right). \tag{60}$$

The metallization on the back of the bottom layer leads here to the simple relation

$$\overline{\mathbf{F}} = \hat{\boldsymbol{S}}\overline{\mathbf{F}}_1 \tag{61}$$

with

$$\hat{\boldsymbol{S}} = \sinh\hat{\boldsymbol{k}}_{\overline{y}}\overline{y}\left(\sinh\hat{\boldsymbol{k}}_{\overline{y}}\overline{d}_1\right)^{-1} \tag{62}$$

if $\overline{\mathbf{F}} = \overline{\mathbf{E}}_x$, $\overline{\mathbf{E}}_z$, or $\overline{\mathbf{H}}_y$, and

$$\hat{\boldsymbol{S}} = \cosh\hat{\boldsymbol{k}}_{\overline{y}}\overline{y}\left(\cosh\hat{\boldsymbol{k}}_{\overline{y}}\overline{d}_1\right)^{-1} \tag{63}$$

for $\overline{\mathbf{E}}_y$, $\overline{\mathbf{H}}_x$, and $\overline{\mathbf{H}}_z$.

The function within the open top layer $(n+1)$ following from (32) is

$$\overline{\mathbf{F}}(y) = \hat{\boldsymbol{S}}\overline{\mathbf{F}}_n \tag{64}$$

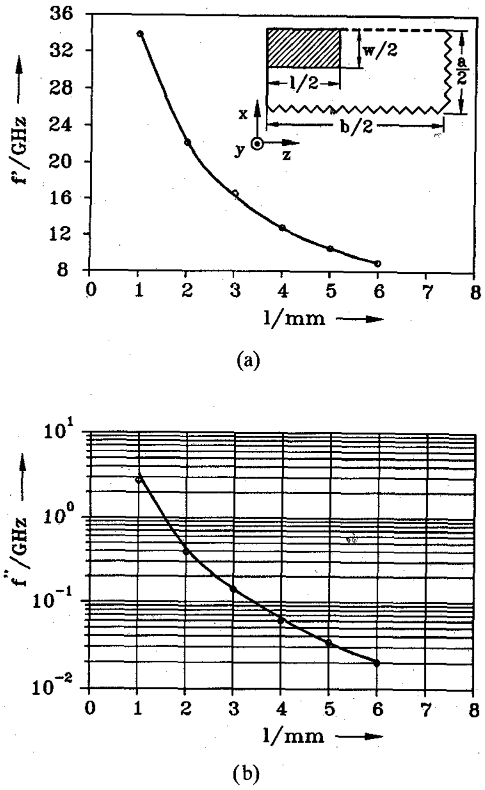

Fig. 5. Real part (a) and imaginary part (b) of the complex resonant frequency $f = f' + jf''$ of a rectangular microstrip patch as a function of length l. ——— MoL, o Nam and Itoh [1]. ($\varepsilon_r = 9.6$, $w = 0.635$ mm, $d = 0.635$ mm. For good convergence, the distance $[a, b]$ between the walls is more than one effective wavelength.)

with

$$\widehat{S} = e^{-\widehat{k}_{\overline{y}}(\overline{y}-\overline{y}_n)}. \quad (65)$$

The sign of the radical must be chosen according to (33).

The field quantities are now transformed back to spatial domain and the Hadamard products are carried out after a straight-line interpolation.

III. Results

A single, rectangular microstrip patch with one dielectric layer of thickness d (Fig. 2) has been investigated. The use of dual boundary conditions makes it possible to add electric or magnetic walls in an easy way to utilize the symmetry of the structure, and to reduce the amount of necessary computer storage. A Taylor series approximation, $p_0 = 1$, $p_2 = 1/2$, has been used for the radical function of the operator on every wall.

Computed results of the complex resonant frequency as a function of the resonator length are presented in Fig. 5(a), (b). They show a very good agreement to those achieved with the integral equation method [1].

The radiated power in the principal planes of the resonator is shown in the vector plots [Fig. 6(a), (b)]. On the magnetic wall ($x = w/2$)

$$p_x = 0 \qquad p_y = e_z h_x^* \qquad p_z = -e_y h_x^* \quad (66)$$

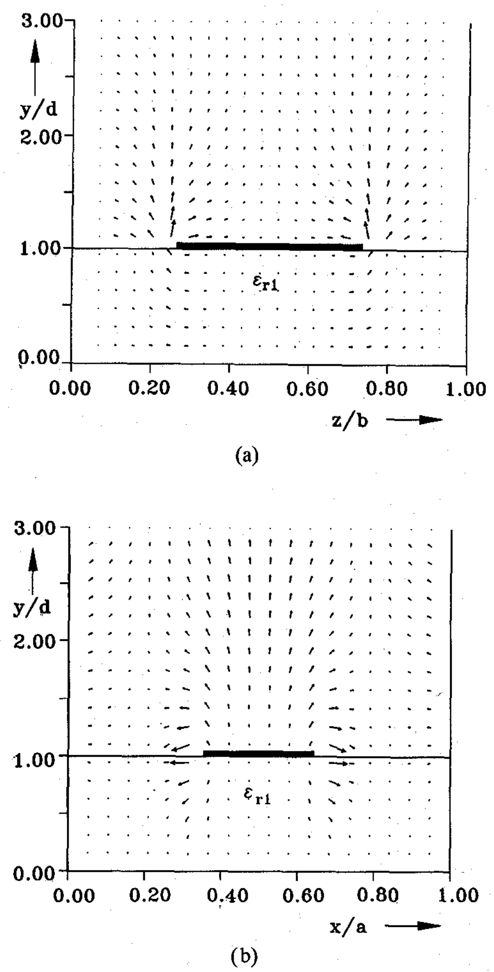

Fig. 6. Energy flow of radiated power in the principal planes of the resonator. (a) $x = w/2$, (b) $z = l/2$. ($d = 1$ mm, remaining data as in Fig. 5.)

and on the electric wall ($z = b/2$)

$$p_x = -e_z h_y^* \qquad p_y = e_z h_x^* \qquad p_z = 0 \quad (67)$$

is valid, and so the computational effort can be reduced significantly. Clearly, we observe the radiating edges in the longitudinal direction, the main beam area perpendicular to the resonator and the excitation of the surface wave.

IV. Conclusion

Introducing absorbing boundaries to the method of lines, radiating devices can be analyzed (as has been shown) by the computation of the complex resonant frequency of a single microstrip patch. The application of the method of lines is simple because no complicated mathematical preparation has to be performed. All field components and the radiated power are known in the whole discretized area, and so it is possible to have a look at near-field phenomena and coupling effects.

Several structures with various shapes and multiple arbitrary thin layers, as applied in hyperthermia and geophysics, can be analyzed (Fig. 7) in the same way, as have already been demonstrated in other publications [4], [2]. Optional metallizations in the interfaces (stacked patches) can be included, and there is no difficulty to consider radiation effects in both vertical directions (Fig. 8). To this end, only an equation

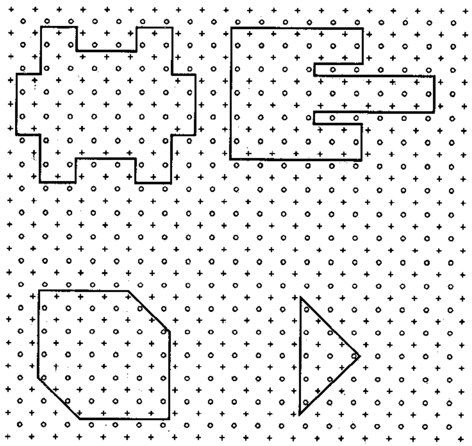

Fig. 7. Examples of microstrip resonators and their discretization with the method of lines.

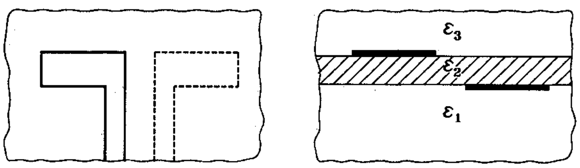

Fig. 8. Patch with radiation in two directions.

similar to (36) has to be taken into account at the interface to the bottom layer.

REFERENCES

[1] S. Nam and T. Itoh, "Calculation of accurate complex resonant frequency of an open microstrip resonator using the spectral domain method," *J. Electromag. Waves Appl.,* vol. 2, no. 9, pp. 635–651, 1988.

[2] R. Pregla and W. Pascher, "The method of lines," in *Numerical Techniques for Microwave and Millimeter-Wave Passive Structures,* T. Itoh, Ed., New York: Wiley, 1989.

[3] U. Schulz and R. Pregla, "A new technique for the analysis of the dispersion characteristics of planar waveguides," *AEÜ,* vol. 34, pp. 169–173, 1980.

[4] S. B. Worm and R. Pregla, "Hybrid-mode analysis of arbitrarily shaped planar microwave structures by the method of lines," *IEEE Trans. Microwave Theory Tech.,* vol. MTT-32, pp. 191–196, Feb. 1984.

[5] W. Pascher and R. Pregla, "Full wave analysis of complex planar microwave structures," *Radio Sci.,* vol. 22, pp. 999–1002, Nov. 1987.

[6] A. Dreher, "The method of lines and the integral equation method for the analysis of planar antennas" (in German), *Fortschritt Berichte,* ser. 21, no. 116, VDI-Verlag GmbH, Düsseldorf, 1992.

[7] A. Dreher and R. Pregla, "Analysis of planar waveguides with the method of lines and absorbing boundary conditions," *IEEE Microwave Guided Wave Lett.,* vol. 1, pp. 138–140, June 1991.

[8] R. Pregla and W. Pascher, "Diagonalization of difference operators and system matrices in the method of lines," *IEEE Microwave Guided Wave Lett.,* vol. 2, pp. 52–54, Feb. 1992.

[9] B. Engquist and A. Majda, "Absorbing boundary conditions for the numerical simulation of waves," *Math. Comput.,* vol. 31, pp. 629–651, July 1977.

[10] T. G. Moore, J. G. Blaschak, A. Taflove, and G. A. Kriegsmann, "Theory and application of radiation boundary operators," *IEEE Trans. Antennas Propagat.,* vol. AP-36, pp. 1797–1812, Dec. 1988.

[11] J. A. Eisele and R. M. Mason, *Applied Matrix and Tensor Analysis.* New York: Wiley, 1970.

[12] B. T. Smith, J. M. Boyle, J. J. Dongarra, B. S. Garbow, Y. Ikebe, V. C. Klema, and C. B. Moler, *Matrix Eigensystem Routines—EISPACK Guide.* Berlin: Springer-Verlag, 1976.

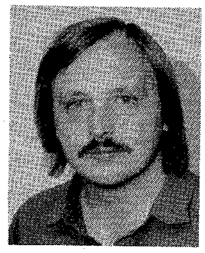

Achim Dreher (M'92) was born in Hermannsburg, Germany, on January 8, 1955. He received the Dipl.-Ing. (M.S.) degree from the Technische Universität Braunschweig, Germany, in 1983, and the Dr.-Ing. (Ph.D.) degree from the FernUniversität in Hagen in 1992, both in electrical engineering.

From 1983 to 1985 he was with Rohde & Schwarz GmbH & Co. KG in München as a Development Engineer. Since 1985 he has been with the FernUniversität in Hagen as a Research Assistant, where he is engaged in numerical techniques for the analysis of planar antennas and microwave structures.

Reinhold Pregla (M'76–SM'83) was born in Luisenthal on August 5, 1938. He received the master's degree in electrical engineering (Dipl.-Ing.) and the doctorate of engineering (Dr.-Ing.) from the Technische Universität Braunschweig, Germany, in 1963 and 1966, respectively.

From 1966 to 1969 he was a Research Assistant in the Department of Electrical Engineering of the Technische Universtät Braunschweig (Institut für Hochfrequenztechnik), where he was engaged in investigations of microwave filters. After the Habilitation, he was a Lecturer in high frequencies at the Technische Universität Braunschweig. Since 1973 he has held the position of Professor at the Ruhr-Universität Bochum, Germany, and since 1975, he has held the position of full Professor in Electrical Engineering at the FernUniversität (a university for distance study) in Hagen, Germany. His fields of investigation include microwave filters, waveguide theory, and antennas.